Journal of Materials and Environmental Sciences
ISSN : 2028-2508
CODEN : JMESCN

J. Mater. Environ. Sci., 2018, Volume 9, Issue 3, Page 946-954

https://doi.org/10.26872/jmes.2018.9.3.105

http://www.jmaterenvironsci.com

The suitability of thermally activated red illite/kaolinitic clay as raw material for geopolymer binders

I. Ben Messaoud *, N. Hamdi, E. Srasra

Physical Chemistry Laboratory for Mineral Materials and Their Applications, National Center for Research in Materials Sciences (CNRSM), B.P.73 – 8020, Soliman, Tunisia

Received 26 Apr 2017,
Revised 12 Jun 2017,
Accepted 19 Jun 2017

Keywords

- ✓ Tunisian clay;
- ✓ Thermal treatment;
- ✓ Geopolymers;
- ✓ Compressive strength

imenbenmessaoud19@gmail.com
(Imen Ben Messaoud)

Abstract

This study evaluates the use of Tunisian hematite rich clay as aluminosilicate source for geopolymer synthesis. The clay fraction was heated at 750 and 950 °C for 2h and then activated by potassium hydroxide and sodium silicate. The heated clay induce various reactivities according to the results obtained by XRD, ^{27}Al MAS-NMR, thermal analysis (DTA), particle size distribution and specific surface area. After geopolymerization, the compressive strength of the hardened geopolymer cement (as an indicator of clay reactivity) increased with the heat treatment. It can be concluded that the most convenient temperature for the heated clays in view of producing geopolymer cements is obviously around 950 °C.

1. Introduction

In the past three decades, urbanization has proceeded faster in developing countries. Ordinary Portland Cement (OPC) based materials such as concrete are nowadays the most widely used construction materials. Unfortunately, the cement industry accounts for around 4% of the total global greenhouse gas emissions and up to 8% of the total global anthropogenic CO_2 emissions [1]. It has become a major environmental issue.

Geopolymer cement is considered to be the most effective ways of reducing the environmental impact of the cement industry. These eco-materials can be synthesized by the alkaline activation of aluminosilicates at room temperature and providing a low cost, fast setting, low permeability, resistance to fire and acid attack [2], ability to radically decrease the heavy metal ions mobility [3], great resistance to freeze thaw cycles, and good compressive strength resistance [4].

The properties of geopolymer materials are mainly affected by the aluminosilicate source [5], [6]. Granulated blast furnace slag from iron production and fly ash from coal combustion of electricity production are being used to synthesis geopolymer materials [5], [6]. Nevertheless, there is an interest to search for alternative to these aluminosilicate sources due to supply-and-demand concerns in the future. One of the most promising alternative sources are raw clays as they are an abundant and widespread material that can lower transportation costs. Furthermore, the production process of calcined clay is less energy intensive due to lower heating temperatures and the absence of a decorbonation reaction. The calcination process of kaolinite arises in the temperature range of 500 and 850 °C [7], [8] resulting in the dehydroxylation of the clay and the formation of an amorphous phase. Nevertheless, calcination to higher temperatures can induce the formation of new unreactive phases such as mullite [9]. In any case, a careful calcination method can activate the clay and leads to an increase of its geopolymeric reactivity. Various studies have already demonstrated the efficiency of calcined clays to produce geopolymer materials [8], [10]. For instance, Nmiri et al.[11] calcined a Tunisian kaolinitic clay at the temperature range of 550, 700, 900 and 1100 °C for 2 and concluded that the best calcination temperature for geopolymer synthesis is 700 °C. However, calcined clays other than metakaolin are sparsely used due to the presence of iron oxide, as is the case for Medenine clay. Hence, this study examines the reactivity of unheated and calcined clays in order to produce geopolymer materials.

2. Materials and methods

2.1. Materials processing

This study used the Tunisian clay as the original material. The clay was sampled from Tejra in southern of Tunisia then heated at 750 and 950°C for 2 hours to transform to metastable state (in term of alumina environment) and quite disordered. Dried clay fraction was crushed and sieved to 106 μm to be useful for characterization of clay fraction and geopolymer synthesis.

The alkaline solution was prepared by mixing sodium silicate and potassium hydroxide solution (15 M) so as to obtain Si/(Na+K) molar ratio of 0.7. The sodium hydroxide solution was obtained by dissolving sodium hydroxide pellets with a purity of 99% in distilled water and sodium silicate (Na_2SiO_3) powder supplied from Fisher company with density of 2.4 $g \cdot cm^{-3}$ and weight ratio SiO_2/Na_2O=2.

2.2. Paste samples preparation

The preparation of geopolymer paste samples consisted of mixing alkaline solution with clay powder according to liquid/solid mass ratio of 3. The fresh geopolymeric paste is rapidly placed into plastic cylindrical moulds with a diameter (Ø) of 16 mm and a height (h) of 32 mm. The samples were vibrated for few minutes on the vibration table to remove entrained air. In order to prevent the evaporation of mixing water and the surface carbonation, the specimens were covered by plastic film during the hardening process. Geopolymer samples were left to cure under ambient temperature (approximately 22°C). The mold is removed after hardening of the specimens. At the end of the curing regime, after 28 days, the samples were dried well at 60°C for 24 h then exposed to compressive strength measurements. .

2.3. Methods

The calcinaton of Tunisian clay was carried out in a programmable electric furnace (Nabertherm) with a heating gradient of 15 °C/min, a soaking time of 2 h, and natural cooling inside the kiln. Some previous studies showed that calcination for 2 h is sufficient to attain the maximum dehydroxylation of the material at temperatures higher than 600 °C [7]. TDA experiment was applied to characterize the raw clay. It was performed in a Pt crucible between 60 and 1200 °C using Setaram Setsys evolution. The samples were heated in dry airflow at a range of 10°C/min. The granulometric analysis of the powder of the raw and heated clay at 750 and 950 °C has been made by laser scattering in aqueous dispersion (Microtrac S 3500).The sample was dispersed using a standard surfactant (Dolapix CE 64) and with ultrasound for 5min. Selected samples were also used for the scanning electron microscopic (SEM) in the aim to analyze morphological features of clay.

BET method using a Quantachrome Autosorb instrument was applied to determinate the specific surface area and the pore volume of raw clay at 77K. The pore parameters were measured on a Micromeritics Autopore II 9215. A Micromeritics Sedigraph 5100 with interface controller was used to obtain the particle size distribution of the clays powder.

Mineralogical analysis of the raw and calcinated clays and geopolymer sample was carried out by X-ray diffraction. The analyses were recorded on Phillips X' Pert diffractometer. The XRD patterns obtained by a scanning rate of 1° per min from 2θ =4° to 60° and steps of 2θ = 0.04°.

Clay and geopolymer materials samples were studied also by ^{27}Al Magic Angle Spinning Nuclear Magnetic Resonance (MAS NMR) using a BRUKER 300WB spectrometer. The ^{27}Al spectra were obtained at resonance frequencies of 78.2 MHz.

Compressive strengths of the hardened geopolymer were tested using a LLOYD EZ50 universal testing machine with a crosshead speed of 3 mm/min.

3. Results and discussion

3.1. Characterization of raw materials

3.1.1. Characteristics of the clay fraction

The mineralogical composition of the raw and calcined clay samples is reported in figure 6. X-ray diffraction pattern shows the presence of quartz (ICCD 01-085-1780), kaolinite (ICCD 01-089-6538), hematite (ICCD 01-087-1164), dolomite (ICCD 01-075-1760), and illite (ICCD 00-002-0050), as principal mineralogical phases for raw clay. According to X-ray diffraction analyses, this material has an important content of kaolinite (53 %), while the impurities represented by illite (29 %) and quartz (14 %) are particularly significant.

The chemical results obtained from the analyses of the unheated clays are reported in Table 1. The chemical composition shows a high amount of silica (55.14 %) and a relatevely low amount of alumina (14.2 %). Furthemore, a considerable amount of Fe_2O_3 present in the clay samples which result in the charcteristic red

color. In addition, the potassium content (2.7 %) is important which suggests the presence of illite. Moreover, clay incorporate some MgO (3.6 %) and CaO (1.7 %), which is probably associated to carbonate earth alkaline compounds. The high ignition loss (LOI) (13 %) is associated to the presence of substantial volatiles [12].

Table 1. Chemical composition of the raw material (wt. %)

Compounds	SiO_2	Al_2O_3	Fe_2O_3	MgO	CaO	Na_2O	K_2O	LOI
Clay	55.14	14.22	8.12	3.65	1.76	0.53	2.73	13.11

The thermogram of clay (fig.1) shows three endothermic phenomena: the first is at approximately 83°C due to the elimination of physisorbed water. The second is at approximately 530°C arises from the structural dehydroxylation of kaolinite. The last endothermic peak at 700°C, related to the decarbonation of dolomite [13]. Moreover, an exothermic peak occurs at approximately 980°C and arises from a structural reorganization, such as the formation of mullite [13], [14].
This result is related to iron oxide that start to diffuse in kaolin from 900 °C provoking the formation of mullite and corroborated with Prud'homme et al., (2013) investigation in which they have proved that at 980 °C, mullite nuclei were observed.

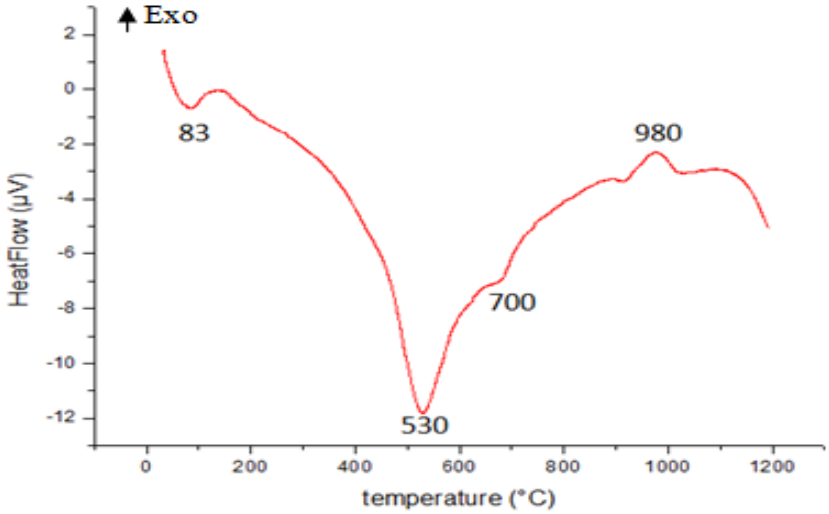

Figure 1: Heat flow curves of the raw clay.

BET specific surface area of clays was measured before and after heat treatment to gain information about the physical changes occurred during the calcinations phase (Table 2). According to these data, raw clay has an important specific surface area of 39 m²/g. This value indicate the disordered state of the clay since the specific surface area of raw kaolinite can be related to the degree of ordering [15].

Table 2. Characteristics of the clays before and after calcination, BET specific surface area and medium size distribution (D_{50}).

	S_{BET} (m^2/g)	**D_{50} (µm)**
Raw clay	**39**	**5**
750°C	**35**	**14**
950°C	**2**	**17**

Calcination temperatures above 750 °C induce a sudden decrease in the specific surface area. Thus, for elevated temperature the particles tend to greater densification resulting in a decrease of the specific surface which is likely due to enhanced sintering phenomena. When the clay was calcined at 950°C, a significant drop in specific surface area from 35 m²/g to 2 m²/g was observed. In fact, increasing calcination temperature results in a small further decrease in the specific surface area due to additional sintering. According to Hollanders et al [16], illitic clays particles tend to agglomerate much more than the kaolinitic clays resulting in a decrease of the specific surface.

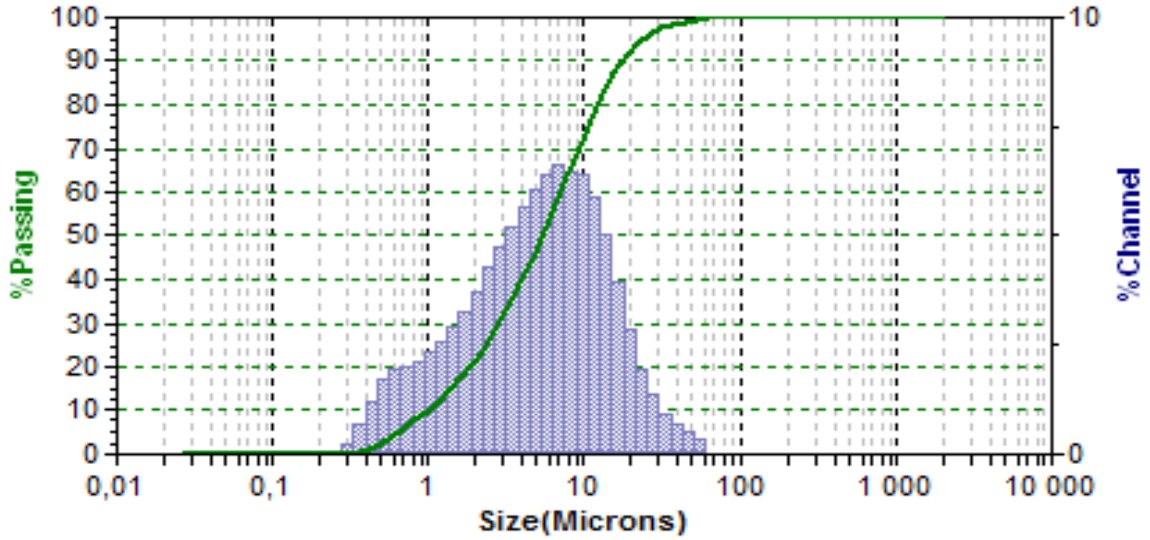

Figure 2: Particle size distribution of the raw clay fraction

Another important modification induced by the thermal treatment is associated to the size of the particles. The raw material represented by a D_{50} of 5 µm (table .2) is characterized by two populations (figure.2). The first with a maximum at around 1 µm (< 2 µm which caracterize clay minerals). The second with a maximum of 10 µm. Hedfi et al [17] that dealt with Tabarka Tunisian Kaolin comfirm taht this increase in the particle size of the clay is due to the agglomeration of the particles.

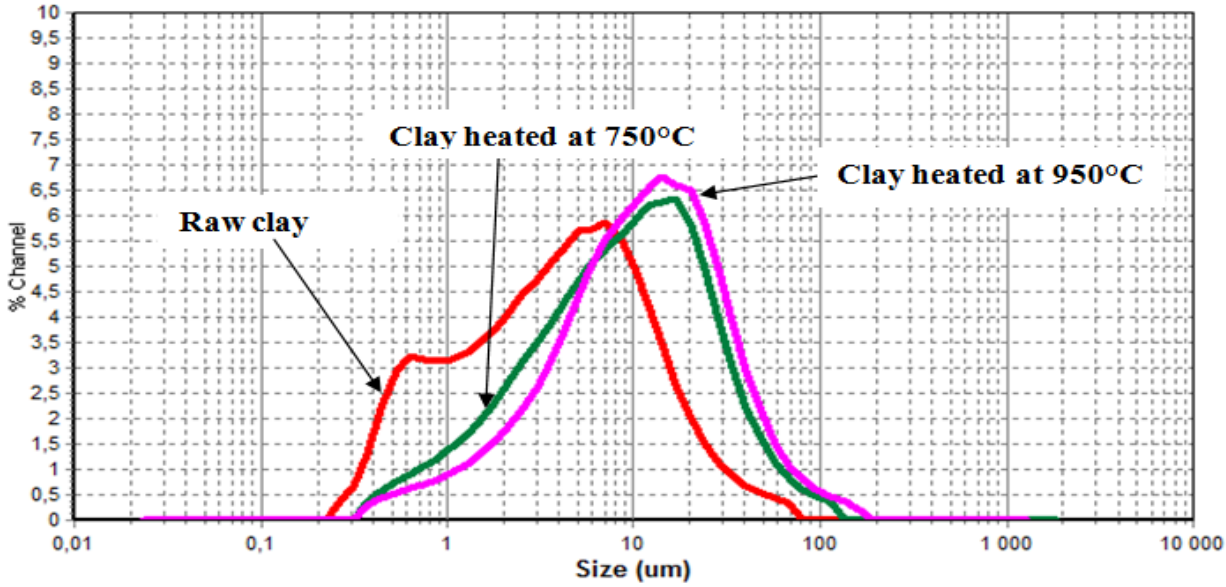

Figure 3: Particle size distribution of the heated clay fraction

The thermal treatments cause physical and mineralogical modifications for the clay fraction. For the clay heated at 750°C and 950°C, the particle size distribution was reduced to one population (figure.3) .The increase of the D_{50} value (table 2) from 5 µm for the unheated material to 17 µm for calcined clay confirms that thermal treatment tends to agglomerate particles together.

SEM micrographs of raw clay show the morphology of the clay particles (fig.4). Clay was composed mainly of thick compact irregular hexagonal particles together with larger lamella of illite and kaolinite. After heat treatment especially at 950 °C (fig.5), the particles became agglomerated due to the partial fusion that corroborate with the previous results. X-ray diffraction pattern for the calcined clay was presented in fig. 6. It is found that the reflections of kaolinite disappeared after increasing temperature up to 750 °C. At this temperature the kaolin was transformed to the amorphous metakaolin indicating its destruction in (001) direction [18].

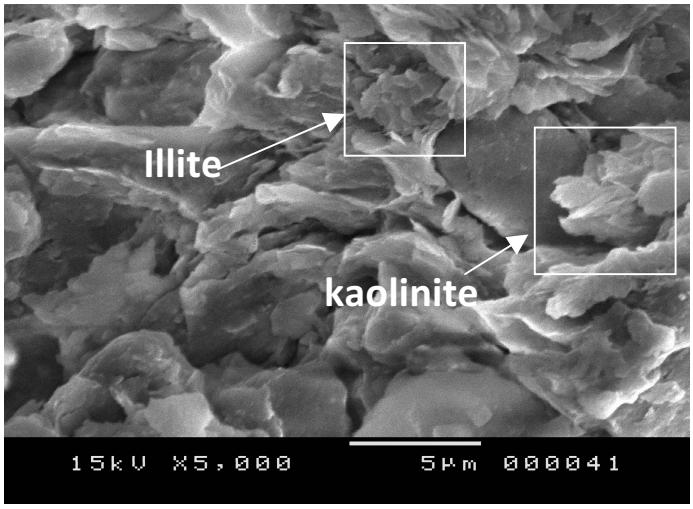

Figure 4: SEM micrographs of raw clay

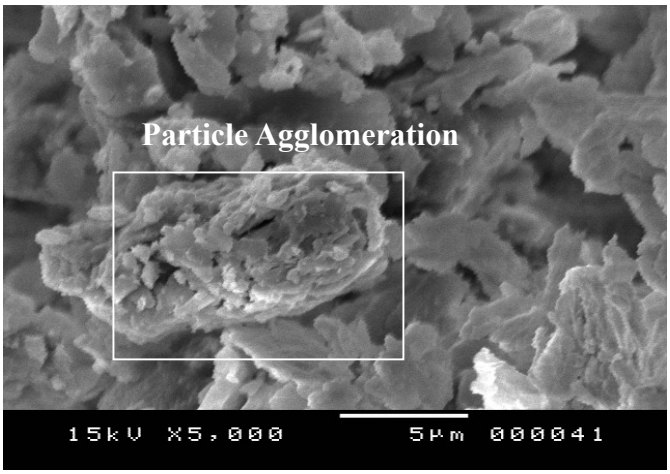

Figure 5: SEM micrographs of clay heated at 950°C

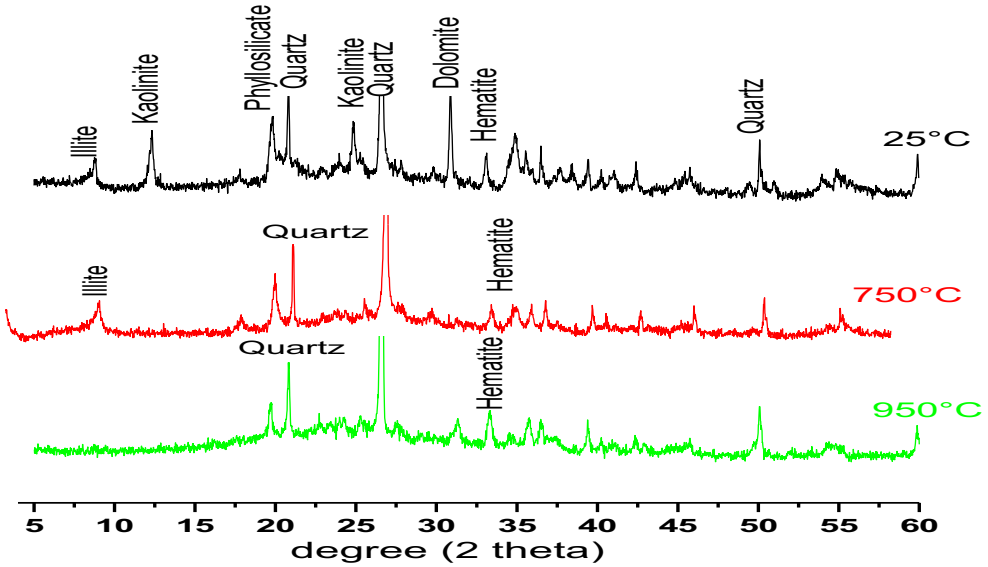

Figure 6: XRD patterns of the raw and calcined clay samples at 750 and 950 °C

Concerning illite reflections, no significant changes were detected at 750°C, because of its higher thermal stability [19].

At 950 °C, illite reflection is no longer detected in the X-ray diffractograms. Calcination at higher temperatures decrease the amounts of stable crystalline phases at the expense of amorphous phases [20]. On the other hand,

the reflections of hematite and quartz persist at this temperatureIn order to get more quantitative and qualitative details about the raw clay, oriented clay slides were analyzed and the results are shown in Fig.7.
The reflections at d_{001} = 7, 2 Å and d_{002} = 3.56 Å disappear after heating to 550 °C which confirms the presence of the kaolinite phase in the clay fraction. The basal reflection corresponding to kaolinite and illite observed at approximately d_{001} = 7, 2 Å and d_{001} = 10 Å respectively remain unchanged for the glycolated sample. These results reflect the inaccessibility of the interlayer spaces of this aluminosilicate to the ethylene glycol entities. As a consequence the Medenine clay is non-swellable clay. In addition, the decrease in intensity of the illite indicates the decrease in the interlayer spaces of the silicate due to dehydration

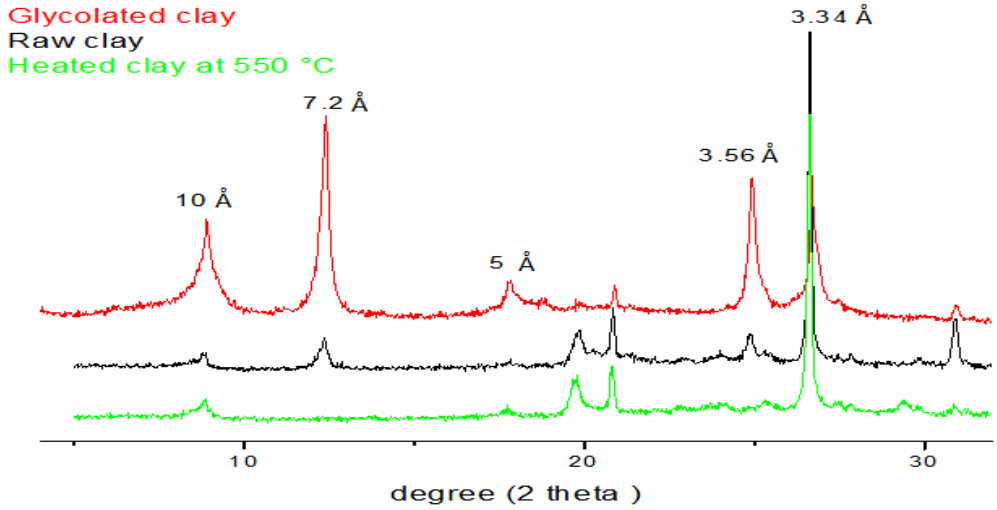

Figure 7: DRX of the raw Medenine clay, heated clay at 550 °C and treated with ethylene glycol.

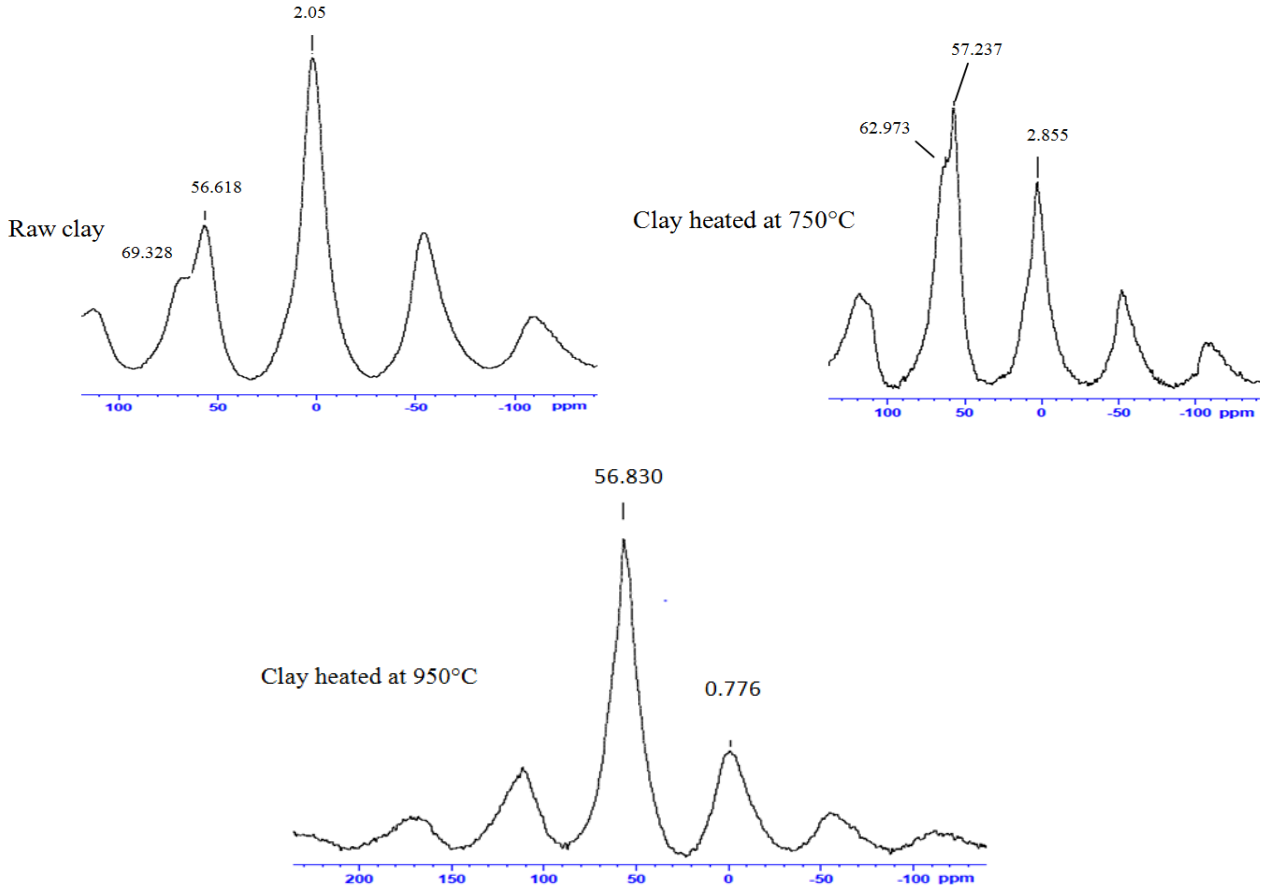

Figure 8: ^{27}Al NMR spectra of raw clay and clay heated at 750 and 950°C

The ^{27}Al spectrum of Tunisian red raw clay consisted of two resonances (Fig. 8). The ^{27}Al NMR spectrum of raw clay is dominated by the resonance from Al in octahedral coordination around 2.05 ppm which can be

attributed to Al^{VI} in illite and kaolinite [13]. Another peak at 69 ppm was assigned to tetrahedral Al^{IV}.
The most important information about the structure of the clay after heat treatment comes from the coordination number of Al atoms [22]. The presence of 6-Al and 5-Al at 750 °C reveals the dehydroxylation process of the kaolinite. This intermediate is common when kaolinite transforms to metakaolinite [13]. Heated at higher temperatures, the coordination number of Al atoms of the clay is converted from 6 (2 ppm) to 4 (62- 69 ppm), with Al^{V} and Al^{IV} developing simultaneously [23]. According to different investigators involving various samples and under different thermal treatments, the reactivity of metakaolinite is at a maximum when the content of Al^{VI} is at a minimum [23]. With regard to the hexa-coordinated Al, there is a shift of the band from 2 ppm to -0.77 ppm. This fact reflects the possible presence of non-dehydroxylated clay and partially altered clay [23].

3.2. Characterization of geopolymer samples

The X-ray diffractograms of geopolymer pastes (Fig. 9) show that the basal reflection (001) of non-dehydroxylated kaolinite at 7 Å initially present in raw clay disappears after alkaline treatment for the geopolymer sample. In addition, the intensity of the basal (001) reflection of illite near 10 Å shows a small decrease after geopolymerization reaction. These results indicate that the silicate crystal structure of the clay is partially altered after alkaline treatment proving that clay minerals are selectively dissolved in alkaline media. However, the comparison between Figs. 6 and 9 revealed certain changes with regard to the halo peak representing the amorphous phase. In addition, the reflection of quartz and hematite still remain in the geopolymer samples. These impurities were not altered by the geopolymerization reaction. Essaidi, N. et al [24] demonstrate that there is no interaction between the iron oxide and the potassium hydroxide during geopolymerization reaction. Thus, iron oxide does not contribute in the formation of geopolymer materials. Therefore, the silicate species containing KOH ruin around the particles of hematite non altered and lead to the formation of different specific networks other than geopolymer network in final materials. These varieties of networks act as a reinforcing load and cause the improvement of mechanical properties. Furthermore, the X-ray diffractograms of geopolymer pastes revealed the shift of the halo peak from 18° - 30° for unheated and calcined clay (Fig. 6) to 20° and 45° for geopolymer samples (Fig. 9) indicating the developing the geopolymer reaction for these samples.

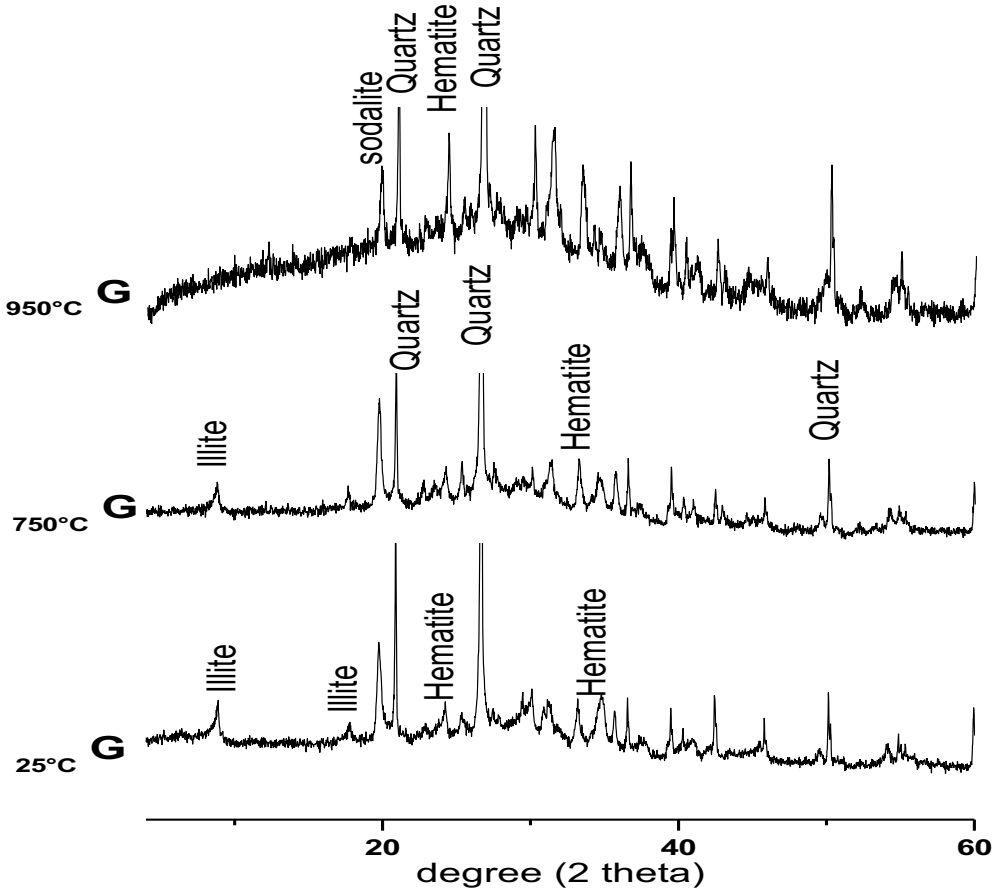

Figure 9: XRD patterns of geopolymers.

There was a clear correlation between the compressive strength of geopolymer samples and the grain size (D_{50}) of clay (Fig. 10). Thus, when the particle of the clay was more agglomerated, compressive strength of geopolymer samples was more important. On the other hand, the rise in compressive strength with the elevation in calcinations temperature was influenced essentially by the dehydroxylation of residual minerals contained in clay [25]. It is well known that to produce geopolymers, amorphous phase present the reactive phase in alkaline medium. Thus, normally at the temperature of calcinations of 750°C where the dehydroxylation of the kaolin was achieved, geopolymer samples will gain the maximum value of the compressive strength. However, the results obtained after compressive strength test of the geopolymer samples aged after 28 days show that samples prepared with clay calcined at 950°C were more resistance to the compressive test than samples prepared with clay calcined at 750°C. According to RMN analyses (fig.8), the disorder state of the Tunisian clay induced by the thermal treatment at 950°C is the more important than for the thermal treatment at 750°C. These results lead up to consider that during geopolymer synthesis, increase compressive strength with respect to the temperature of calcination is regulated by the amorphous phase.

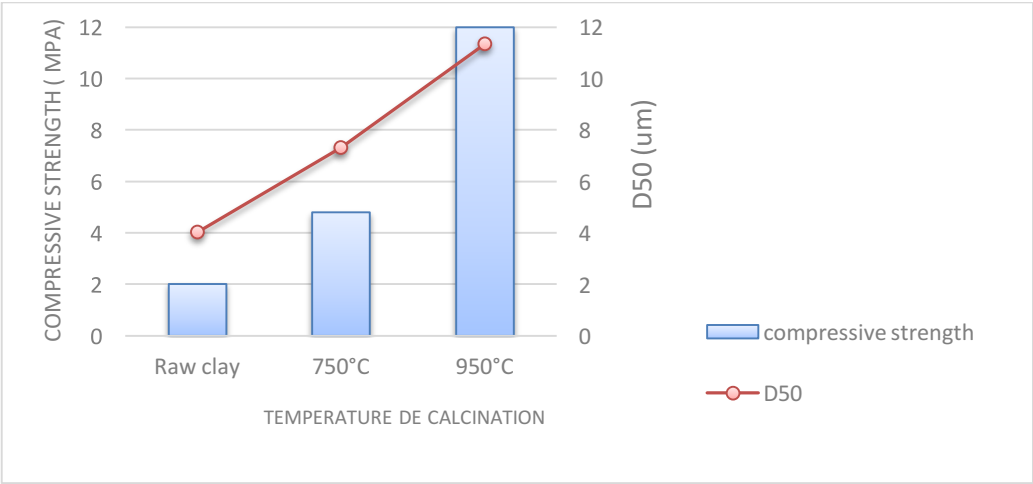

Figure 10: Variation of compressive strength of geopolymer samples and D_{50} of the clay used for the geopolymer synthesis

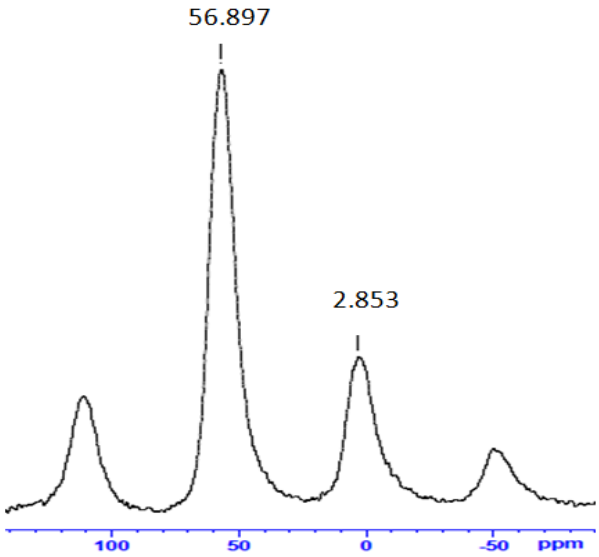

Figure 11: ^{27}Al NMR spectra of geopolymer material based on heated at 950°C.

Fig. 11 shows the ^{27}Al NMR spectra of geopolymer foam synthesized from clay heated at 950°C. The spectra display a primary dominant band at 56.9 ppm, characteristic of a for-coordinated Al environment and implies the formation of geopolymer gel in the geopolymer samples [26]. A weak band associated with hexa-coordinated Al at 2 ppm reveals that a small amount of octahedral aluminum is still present in the materials derived from non-dehydroxylated kaolinite and/or an illite phase [27]. Compared to calcined clay, the intensity of ^{27}Al band at 56.9 ppm was increased whereas the intensity of band at 2 ppm decreased. These results clearly

indicate a large degree of polycondensation regardless of the metakaolins used. Interestingly, the Al^{IV}, which appears in raw metakaolins, is transformed into Al^{IV} in the geopolymerization reactions [28]. In fact, six-coordinated aluminum species present in the raw material had condensed to form the three-dimensional geopolymeric network that essentially consisted of four-coordinate aluminum species [19].

Conclusion

Red illitic-kaolinitic Tunisian clay was heated at 750 and 950 °C for two hours. Raw and heated clay were used to produce geopolymer binders. After heat treatment, the structural evolution of clay was studied by, XRD, BET, SEM, ^{27}Al MAS-NMR and particle size distribution. With the rise of temperature, the clay particles tend to agglomerate and induce a decrease in the specific surface area and an increase in medium size distribution (D_{50}**)**. According to ^{27}Al MAS-NMR, the heat temperature of 950°C offers better reactive clay for the geopolymer synthesis. This result corroborates with the compressive strength test.
For geopolymerazition reaction, clay minerals are selectively dissolved in alkaline media. Increase compressive strength with respect to the temperature of calcination is regulated not only by an amorphous phase but also by the presence of quasi no reactive phases in the clay such as hematite.

References

1. L. Barcelo, J. Kline, G. Walenta, and E. Gartner*, Mater. Struct*., 47 (2013) 1055.
2. T. Bakharev, Cem. Concr. Res., vol. 35 (2005) 658.
3. Q. Li, Z. Sun, D. Tao, Y. Xu, P. Li, H. Cui, and J. Zhai, *J. Hazard. Mater*., 262 (2013) 325.
4. K. Al-Zboon, M. S. Al-Harahsheh, and F. B. Hani, *J. Hazard. Mater*., 188 (2011) 414.
5. M. O. Yusuf, M. A. M. Johari, Z. A. Ahmad, and M. Maslehuddin, *Constr. Build. Mater.*, 50 (2014) 361.
6. M. Olivia and H. Nikraz, Mater. Des., 36(2012) 191–198.
7. B. Fabbri, S. Gualtieri, and C. Leonardi, *Appl. Clay Sci.*, 73(2013) 2.
8. A. Elimbi, H. K. Tchakoute, and D. Njopwouo, *Constr. Build. Mater*., 25 (2011) 2805.
9. E. Escalera, R. Tegman, M. L. Antti, *Appl. Clay Sci*., 101 (2014) 100.
10. M. B. Ogundiran and O. J. Ikotun, Trans. *Indian Ceram. Soc*., 73 (2014) 138.
11. A. Nmiri, N. Hamdi, M. Duc, and E. Srasra, *J. Mater. Environ. Sci* , 8 (2017) 276.
12. A. H. Rankin, 51 (1987) 517.
13. N. Essaidi, B. Samet, S. Baklouti, and S. Rossignol*, Appl. Clay Sci*., 88 (2014) 221.
14. E. Prud'homme, A. Autef, N. Essaidi, P. Michaud, B. Samet, E. Joussein, and S. Rossignol, *Appl. Clay Sci*., 73 (2013) 26.
15. E. Galan, P. Aparicio, I. Gonzalez, and A. Miras, *Clay Miner.*, 33 (1998) 65.
16. S. Hollanders, R. Adriaens, J. Skibsted, Ö. Cizer, and J. Elsen*, Appl. Clay Sci.*, 133 (2016) 1.
17. I. Hedfi, N. Hamdi, E. Srasra, and M. A. Rodríguez, *Appl. Clay Sci.*, 101 (2014) 574.
18. M. a. Soleimani, R. Naghizadeh, a. R. Mirhabibi, and F. Golestanifard, " *Iran. J. Mater. Sci. Eng*., 9 (2012) 43.
19. C. Ferone, B. Liguori, I. Capasso, F. Colangelo, R. Cioffi, E. Cappelletto, and R. Di Maggio, *Appl. Clay Sci.,* 107 (2015) 195.
20. T. Seiffarth, M. Hohmann, K. Posern, and C. Kaps*, Appl. Clay Sci.,* 73 (2013) 35.
21. S. N. Monteiro and C. M. F. Vieira, *J. Mater. Process. Technol*., 27 (2009) 2812.
22. T. Watanabe, H. Shimizu, K. Nagasawa, H. Saito, and A. Masuda, *Clay Miner*., 22, (1987) 37.
23. A. Autef, E. Joussein, G. Gasgnier, S. Pronier, I. Sobrados, J. Sanz, and S. Rossignol, *Powder Technol*., 250 (2013) 33.
24. N. Essaidi, B. Samet, S. Baklouti, and S. Rossignol, *Ceram. - Silikaty*, 58(2014) 1.
25. A. R. Sakulich, E. Anderson, C. Schauer, and M. W. Barsoum, *Constr. Build. Mater.,* 23 (2009) 2951.
26. S. J. Lyu, Y. H. Hsiao, T. T. Wang, T. W. Cheng, and T. H. Ueng, *Cem. Concr. Res.*, 54 (2013) 199.
27. Q. Wan, F. Rao, and S. Song, J. Non. Cryst. Solids, 460 (2017) 74.
28. P. Duxson, a. Fernández-Jiménez, J. L. Provis, G. C. Lukey, a. Palomo, and J. S. J. Van Deventer, *J. Mater. Sci.,* 42 (2007) 2917.